Polymer Journal (2017) 49, 141–148

www.nature.com/pj

ORIGINAL ARTICLE

Semi-crystalline A_1–D–A_2-type copolymers for efficient polymer solar cells

Thanh Luan Nguyen[1,5], Hyosung Choi[2,5], Seo-Jin Ko[3], Taehyo Kim[3], Mohammad Afsar Uddin[1], Sungu Hwang[4], Jin Young Kim[3] and Han Young Woo[1]

A series of acceptor$_1$–donor–acceptor$_2$ (A_1–D–A_2)-type copolymers was designed and synthesized using thiophene as an electron-rich unit and benzothiadiazole (BT) and benzotriazole (BTz) as electron-deficient moieties. A weaker acceptor, BTz, was incorporated as a solubilizing moiety with three tetradecyl (or tetradecyloxy) side chains, and a stronger acceptor, BT, was substituted with different numbers of fluorines to modulate the intramolecular charge transfer interaction and the resulting electronic structures. The similar molecular structures of BT and BTz did not disrupt the interchain organization significantly, and the absence of solubilizing alkyl substituents on the electron-rich thiophene did not increase the highest occupied molecular orbital of the resulting polymers. The polymers showed broad absorption in the range of 350–750 nm. Intra- and/or interchain non-covalent coulombic interactions (for example, dipole–dipole interactions via S···O, S···F) ensured a planar backbone and a semi-crystalline morphology in the film. Bulk heterojunction polymer solar cells were fabricated using blends of the polymers and phenyl-C_{71}-butyric acid methyl ester ($PC_{71}BM$). For a difluoro-BT containing polymer (BTzDT2FBT), a power conversion efficiency up to 7% was achieved with a short circuit current density of 14.64 mA cm^{-2}, open circuit voltage of 0.75 V and fill factor of 0.64.

Polymer Journal (2017) **49,** 141–148; doi:10.1038/pj.2016.88; published online 21 September 2016

INTRODUCTION

In recent years, polymer solar cells (PSCs) have been the subject of extensive study because of their potential applicability in light weight, low cost, solution-processable, large-area and flexible photovoltaic devices.[1] Although remarkable progress has been made in PSCs, with successful demonstrations of power conversion efficiency (PCE) of over 10% over the past several decades,[2,3] several challenges remain, such as the synthesis of high-performance photovoltaic polymers with high photostability and minimal batch-to-batch variation, device operational stability and eco-friendly processing for mass production.[4]

To improve the photovoltaic performance of PSCs, tremendous efforts have been devoted to the synthesis of new *p*-type conjugated polymers and *n*-type accepting materials, optimization of processing techniques and adoption of new device architectures.[2,3,5–14] In the design of ideal photovoltaic polymers, broad and strong absorption in the visible to near-infrared region, deep highest molecular orbital (HOMO), high hole mobility and crystalline morphology with appropriate miscibility with fullerenes must be considered together to improve the short circuit current density (J_{SC}), open circuit voltage (V_{OC}) and fill factor (FF). Copolymers (or terpolymers), which comprise two different electron-rich units and one electron-deficient unit[15–17] or one electron-rich unit and two different electron-deficient units,[18–25] are a promising candidate to broaden the absorption of the solar spectrum. The intelligent combination of electron-deficient and electron-rich moieties with different electron-withdrawing or electron-donating strengths is critical to achieve complementary and broad light absorption, thus maximizing photon harvesting.

Benzothiadiazole (BT) is a commonly used strong electron-accepting moiety, in which the 5- and 6-positions on BT can be modified by introducing electronegative substituents such as fluorine and nitrile groups, thus modulating the electronic structures and intra- and/or interchain dipole–dipole interactions of the resulting polymers.[26–28] Single junction devices based on BT containing polymers have achieved PCE of over 10%.[2] Benzotriazole (BTz) has also been studied intensively for PSCs and organic field-effect transistors because of its chemical versatility with three chemically functionalizable sites.[29–36] The central nitrogen can be functionalized with an alkyl chain (to endow solution processability), which separates from the conjugated backbone to reduce steric hindrance, thereby enhancing the effective intrachain π-conjugation and interchain packing. The 5- and 6-positions on BTz can also be modified by introducing electron-withdrawing substituents (for example, fluorine,

[1]Department of Chemistry, College of Science, Korea University, Seoul, Republic of Korea; [2]Hanyang University, Seoul, Republic of Korea; [3]Department of Energy Engineering, Ulsan National Institute of Science and Technology (UNIST), Ulsan, Republic of Korea and [4]Department of Nanomechatronics Engineering, Pusan National University, Miryang, Republic of Korea
[5]These authors contributed equally to this work.
Correspondence: Professor JY Kim, Department of Energy Engineering, Ulsan National Institute of Science and Technology (UNIST), Ulsan 689-798, Republic of Korea.
E-mail: jykim@unist.ac.kr
or Professor HY Woo, Department of Chemistry, College of Science, Korea University, Seoul 02841, Republic of Korea.
E-mail: hywoo@korea.ac.kr
Received 30 June 2016; revised 5 August 2016; accepted 8 August 2016; published online 21 September 2016

nitro, nitrile) or an electron-donating substituent (that is, alkoxy) to modulate the electronic structure and intra- and/or interchain interactions of the resulting polymers. In addition, the introduction of solubilizing alkyl (or alkoxy) substituents onto the electron-deficient unit increases the HOMO energy level negligibly without decreasing the V_{OC} value.[37]

In this study, we report acceptor$_1$–donor–acceptor$_2$ (A_1–D–A_2)-based copolymers that contain electron-rich thiophene and two electron-deficient moieties of BT and BTz in the polymeric backbone. Two solubilizing alkoxy side chains at the 5- and 6-positions of BTz induce intra- and/or interchain coulombic interactions via $S^{\delta+}$—$O^{\delta-}$ between the oxygen and sulfur atoms in the neighboring thiophene and BTz moieties.[38,39] The BT moiety is used as the main acceptor, with fluorine atoms at the 5- and 6-positions to modulate the frontier orbital levels and oxidational stability of the resulting polymers.[40,41] This design is expected to yield both a low band gap and a deep HOMO level. In addition, fluorine substitution is an effective way to increase the crystalline ordering through intra- and/or interchain C-F---H, F---S and C-F---π_F non-covalent attractive interactions.[10,42–44] The similar molecular structure of BT and BTz may induce strong interchain organization, and the absence of solubilizing alkyl substituents on the electron-rich thiophene does not increase the HOMO level of the resulting polymers. The polymers showed broad light absorption covering up to ~750 nm, and strong interchain π–π stacking was clearly observed in the grazing incidence wide-angle X-ray scattering (GIWAXS) measurements. The bulk heterojunction (BHJ) devices based on the blends of A_1–D–A_2 copolymers and phenyl-C_{71}-butyric acid methyl ester ($PC_{71}BM$) exhibited the highest PCE of up to 7% in a conventional single cell architecture.

MATERIALS AND METHODS

A microwave reactor (Biotage Initiator, Biotage, Seoul, Korea) was used to synthesize the polymers. ^{1}H and ^{13}C nuclear magnetic resonance (NMR) spectra were recorded on a JEOL (JNM-AL300) FT NMR system operating at 300 and 75 MHz, respectively. UV–vis spectra were obtained using a JASCO V-630 spectrophotometer (JASCO, Seoul, Korea). The number- and weight-average molecular weights of the polymers were determined by gel permeation chromatography (GPC) with *o*-dichlorobenzene as the eluent at 80 °C on Agilent GPC 1200 series, relative to polystyrene standards. Cyclic voltammetry experiments were performed using a Versa STAT 3 analyzer (AMETEK Scientific Instruments, Seoul, Korea). All cyclic voltammetry measurements were carried out in 0.1 M tetrabutylammoniumtetrafluoroborate (Bu_4NBF_4) in acetonitrile with a conventional three-electrode configuration employing a platinum wire as the counter electrode, platinum electrode coated with a thin polymer film as the working electrode, and a Ag/Ag$^+$ electrode as the reference electrode (scan rate: 50 mV s^{-1}). Thermogravimetric analysis (TGA) and differential scanning calorimetry (DSC) measurements were performed using the 2050 TGA V5.4 A and DSC Q200 V24.4 instruments, respectively, under a nitrogen atmosphere at heating and cooling rates of 10 °C min^{-1}. Atomic force microscopy measurements were carried out using an Asylum MFP-3D atomic force microscope (Oxford Instruments, Santa Barbara, CA, USA) in tapping mode. GIWAXS measurements were conducted at the PLS-II 9A U-SAXS beam line of Pohang Accelerator Laboratory, Korea. High-resolution mass spectrometry was performed with Finnigan MAT 95 XP (Thermo Fisher Scientific, Busan, Korea).

Synthesis of monomers and polymers

The monomers (M1–M4) were prepared by modifying the procedures reported previously.[10,36]

4,7-Bis(5-trimethylstannylthiophen-2-yl)-benzo[c][1,2,5]thiadiazole (M1). Yield: 90%. ^{1}H NMR (300 MHz, $CDCl_3$): δ (p.p.m.) 8.17 (d, J = 3.45 Hz, 2H), 7.87 (s, 2H), 7.29 (d, J = 3.45 Hz, 2H), 0.43 (s, 18H). ^{13}C NMR (75 MHz, $CDCl_3$): δ (p.p.m.) 152.5, 144.9, 140.3, 136.1, 128.2, 125.8, 125.7, −8.14. HRMS ($C_{20}H_{24}N_2S_3Sn_2$): *m/z* (M^+) = 627.9138.

4,7-Bis(5-trimethylstannylthiophen-2-yl)-5-fluoro-benzo[c][1,2,5]thiadiazole (M2). Yield: 85%. ^{1}H NMR (300 MHz, $CDCl_3$): δ (p.p.m.) 8.30 (d, J = 2.85 Hz, 1H), 8.19 (d, J = 3.30 Hz, 1H), 7.79 (d, J = 12.90 Hz, 1H), 7.32 (d, J = 2.85 Hz, 1H), 7.29 (d, J = 3.30 Hz, 1H), 0.43 (s, 18H). ^{13}C NMR (75 MHz, $CDCl_3$): δ (p.p.m.) 159.4, 157.4, 153.3, 149.6, 143.4, 141.5, 140.9, 137.8, 135.9, 135.0, 130.6, 129.0, 125.5, 116.6, 110.8, −8.4. HRMS ($C_{20}H_{23}F_1N_2S_3Sn_2$): *m/z* ($M^+$) = 645.9046.

4,7-Bis(5-trimethylstannylthiophen-2-yl)-5,6-difluoro-benzo[c][1,2,5]thiadiazole (M3). Yield: 96%. ^{1}H NMR (300 MHz, $CDCl_3$): δ (p.p.m.) 8.33 (d, J = 3.15 Hz, 2H), 7.35 (d, J = 3.15 Hz, 2H), 0.43 (s, 18H). ^{13}C NMR (75 MHz, $CDCl_3$): δ (p.p.m.) 150.6, 149.0, 148.4, 142.6, 137.0, 135.3, 131.5, 111.6, −8.1. HRMS ($C_{20}H_{22}F_2N_2S_3Sn_2$): *m/z* ($M^+$) = 663.8944.

4,7-Dibromo-2-tetradecyl-5,6-bis(tetradecyloxy)-2H-benzo[d][1,2,3]triazole (M4). Yield: 95%. ^{1}H NMR (300 MHz, $CDCl_3$): δ (p.p.m.) 4.73 (t, 2H), 4.11 (t, 4H), 2.14 (m, 2H) 1.88 (m, 4H), 1.11 (m, 6H), 1.40–1.27 (br, 60H), 0.91 (t, 9H). ^{13}C NMR (75 MHz, $CDCl_3$): δ (p.p.m.) 151.5, 140.6, 103.0, 74.8, 57.1, 31.9, 30.3, 30.2, 29.7, 29.6, 29.5, 29.4, 29.3, 29.0, 26.5, 26.0, 22.7, 14.1.

Poly[(2-tetradecyl-5,6-bis(tetradecyloxy)-2H-benzo[d][1,2,3]triazole)-alt-(4,7-di(thiophen-2-yl)benzo[c][1,2,5]thiadiazole)]. In a glove box, monomers M1 (0.144 g, 0.23 mmol), M4 (0.206 g, 0.23 mmol), 4 mol% tris(dibenzylideneacetone)dipalladium(0) and 8 mol% tri(*o*-tolyl)phosphine were added in a 5 ml microwave vial. The vial was sealed, and chlorobenzene (2 ml) was added. The reaction was carried out in a microwave reactor with the following conditions: 10 min at 80 °C, 10 min at 100 °C and 40 min at 140 °C. The polymer was end-capped by reacting with 0.1 equiv. of 2-(tributylstannyl)thiophene for 20 min at 140 °C. The polymer solution was cooled, and 0.2 equiv. of 2-bromothiophene was added by a syringe and further reacted for 20 min at 140 °C. After the reaction was completed, the crude polymer was precipitated into a mixture of methanol:HCl (350 ml:10 ml) and then further purified by Soxhlet extraction with acetone, hexane and chloroform. The polymer solution in chloroform was concentrated under reduced pressure and precipitated into cold methanol. The polymer was filtered off and dried under high vacuum. Yield: 70%. Number-average molecular weight (M_n) = 19 kDa, polydispersity index (PDI) = 2.5. ^{1}H NMR (300 MHz, $CDCl_3$): δ (p.p.m.) 0.8–3.0 (br, 81H), 4.0–4.2 (br, 4H), 4.7–5.2 (br, 2H), 7.0–9.0 (br, 6H).

Poly[(2-tetradecyl-5,6-bis(tetradecyloxy)-2H-benzo[d][1,2,3]triazole)-alt-(5-fluoro-4,7-di(thiophen-2-yl)benzo[c][1,2,5]thiadiazole)]. Yield: 65%. M_n = 23 kDa, PDI = 2.6. ^{1}H NMR (300 MHz, $CDCl_3$): δ (p.p.m.) 0.8–3.0 (br, 81H), 4.0–4.2 (br, 4H), 4.7–5.2 (br, 2H), 7.0–9.0 (br, 5H).

Poly[(2-tetradecyl-5,6-bis(tetradecyloxy)-2H-benzo[d][1,2,3]triazole)-alt-(5,6-difluoro-4,7-di(thiophen-2-yl)benzo[c][1,2,5]thiadiazole)]. Yield: 68%. M_n = 27 kDa, PDI = 3.5. ^{1}H NMR (300 MHz, $CDCl_3$): δ (p.p.m.) 0.8–3.0 (br, 81H), 4.0–4.2 (br, 4H), 4.7–5.2 (br, 2H), 7.0–9.0 (br, 4H).

Photovoltaic device fabrication and characterization. Patterned ITO glass substrates (sheet resistivity: 30 Ω per square) were washed with detergent and ultrasonicated sequentially in deionized water, acetone and 2-propanol. The substrates were dried in an oven for 12 h and then subjected to UV–ozone treatment for 15 min. A solution of poly(3,4-ethylenedioxythiophene):polystyrene sulfonate (PEDOT:PSS, Clevios VP Al 4083, Heraeus, Ulsan, Korea) was spin-coated onto the ITO substrate at 4000 r.p.m. for 40 s and then baked at 140 °C for 10 min. The substrates were transferred to a glove box, and the active layer was spin-coated on the PEDOT:PSS layer from a solution of polymer:$PC_{71}BM$ = 1:1 (w/w) dissolved in chlorobenzene (CB) or mixed solvent of CB and 1,8-diiodooctane (DIO) (97:3 vol%) at 1500 r.p.m. for 60 s. Subsequently, an Al (100 nm) electrode was deposited on top of the active layer under vacuum ($< 10^{-6}$ Torr) using thermal evaporation. The area of the Al electrode defines the active area of the device, that is, 4.5 mm^2. The *J*–*V* characteristics of the solar cells were measured by a Keithley 2400 Source

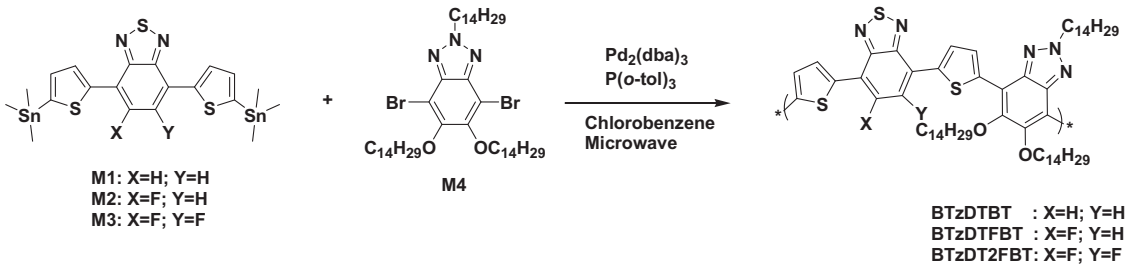

Scheme 1 Synthetic scheme of the polymers.

Table 1 Summary of photophysical, electrochemical and thermal properties of the polymers

Polymer	M_n *(kDa)*[a]	*PDI*	λ_{onset} *(film) (nm)*	E^{opt}_g *(eV)*[b]	*HOMO (eV)*[c]	*LUMO (eV)*[d]	T_d *(°C)*[e]
BTzDTBT	19	2.5	750	1.65	−5.2	−3.55	334
BTzDTFBT	23	2.6	750	1.65	−5.3	−3.65	335
BTzDT2FBT	27	3.5	745	1.66	−5.4	−3.74	338

Abbreviations: BTzDTBT, poly[(2-tetradecyl-5,6-bis(tetradecyloxy)-2H-benzo[d][1,2,3]triazole)-alt-(4,7-di(thiophen-2-yl)benzo[c][1,2,5]thiadiazole)]; BTzDTFBT, poly[(2-tetradecyl-5,6-bis (tetradecyloxy)-2H-benzo[d][1,2,3]triazole)-alt-(5-fluoro-4,7-di(thiophen-2-yl)benzo[c][1,2,5]thiadiazole)]; BTzDT2FBT, poly[(2-tetradecyl-5,6-bis(tetradecyloxy)-2H-benzo[d][1,2,3]triazole)-alt-(5,6-difluoro-4,7-di(thiophen-2-yl)benzo[c][1,2,5]thiadiazole)]; HOMO, highest occupied molecular orbital; LUMO, lowest unoccupied molecular orbital; PDI, polydispersity index.
[a]Number-average molecular weight (M_n) determined by GPC.
[b]Optical band gap in film.
[c]HOMO level was estimated from the tangential onset of oxidation (E_{ox}^{onset}) by cyclic voltammetry. HOMO (eV) = $-(E_{ox}^{onset} - E^{1/2}_{ferrocene} + 4.8)$.
[d]LUMO level was estimated from the HOMO value and optical band gap of the film.
[e]Decomposition temperature (T_d) was determined by TGA at 5% weight loss.

Measurement Unit. The solar cell performance was tested with an Air Mass 1.5 Global (AM 1.5 G) solar simulator (Keithley Instruments, Ulsan, Korea) with an irradiation intensity of 100 mWcm^{-2}. External quantum efficiency (EQE) measurements were performed using the PV measurement QE system by applying monochromatic light from a xenon lamp under ambient conditions. The monochromatic light intensity was calibrated using a Si photodiode and chopped at 100 Hz. All devices were tested under ambient conditions after UV-epoxy encapsulation. For calculating hole and electron mobilities, we also fabricated hole- and electron-only devices with configurations of ITO/PEDOT:PSS/active layer/Au and fluorine-doped tin oxide/active layer/Al, respectively. We obtained hole and electron mobilities by measuring *J–V* characteristics under the dark by using the space-charge-limited current (SCLC) method. The potential loss due to the series resistance of ITO and the built-in potential were carefully considered to ensure accuracy in the measurements.

RESULTS AND DISCUSSION

Molecular design and synthesis

Three different types of A_1–D–A_2 copolymers containing BTz and BT as electron-deficient moieties, that is, poly[(2-tetradecyl-5,6-bis(tetradecyloxy)-2H-benzo[d][1,2,3]triazole)-alt-(4,7-di(thiophen-2-yl)benzo[c][1,2,5]thiadiazole)] (BTzDTBT), poly[(2-tetradecyl-5,6-bis(tetradecyloxy)-2H-benzo[d][1,2,3]triazole)-alt-(5-fluoro-4,7-di(thiophen-2-yl)benzo[c][1,2,5]thiadiazole)] (BTzDTFBT) and poly[(2-tetradecyl-5,6-bis(tetradecyloxy)-2H-benzo[d][1,2,3]triazole)-alt-(5,6-difluoro-4,7-di(thiophen-2-yl)benzo[c][1,2,5]thiadiazole)] (BTzDT2FBT), were synthesized at 65–70% yields by the microwave-assisted Stille coupling reaction of bisstannylated 4,7-di(thiophen-2-yl)benzo[c][1,2,5]thiadiazole (DTBT) derivatives (M1–M3) and 4,7-dibromo-2-tetradecyl-3,4-dibromo-5,6-bis(tetradecyloxy)-2H-benzo[d][1,2,3]triazole (M4) using $Pd_2(dba)_3$ as a catalyst in chlorobenzene (Scheme 1). The BT and BTz moieties were selected because the similar chemical structure of BT and BTz may not disrupt significantly the interchain packing between neighboring polymer chains.

Three different A_1–D–A_2 copolymers were designed by considering the chain planarity via intrachain non-covalent coulombic interactions (such as $S^{\delta+}\cdots F^{\delta-}$and $S^{\delta+}\cdots O^{\delta-}$), solubility and adjustment of the frontier orbital energy levels by incorporating electron-withdrawing fluorine atoms. Two types of electron-deficient BTz and BT units were incorporated in the polymeric main chain, where the BTz moiety is a relatively weaker acceptor (A_1) compared with BT (A_2). In the molecular structure of BTzDTBT series polymers, the weaker acceptor BTz was utilized as a solubilizing moiety, where the 2(N) and 5, 6(C) positions were alkylated with multiple tetradecyl (or tetradecyloxy) side chains for solution processability. The stronger acceptor BT was functionalized with different numbers of electronegative fluorine atoms to finely modulate the HOMO level which strongly influences the V_{OC} of photovoltaic devices. Moreover, all of the solubilizing alkyl (or alkoxy) chains were incorporated at the electron-deficient acceptor (BTz) moiety. The HOMO level is mainly determined by the electron-rich thiophene moiety, and the absence of electron-releasing alkyl (or alkoxy) substituents on thiophene may not increase the HOMO level, affording a deep HOMO level and a high V_{OC}.[45] More importantly, the alkoxy groups at the 5, 6-positions of BTz and fluorine atoms at the 5, 6-positions of BT can increase the chain planarity with minimized torsional angle in the main backbone via $S^{\delta+}\cdots F^{\delta-}$and $S^{\delta+}\cdots O^{\delta-}$ coulombic dipole–dipole interactions, thereby improving interchain ordering and charge–carrier transport.[10,45] Computational studies using density functional theory (DFT, Jaguar quantum chemistry software, M06–2X/6–31G** level) were also performed.[46,47] The tetradecyl and tetradecyloxy substituents were replaced with a methoxy group to simplify the calculations. The introduction of alkoxy substituents on BTz was observed to minimize the torsional angle (6–7°) via the $S^{\delta+}\cdots O^{\delta-}$ non-covalent attractive interactions (Supplementary Figure 1). Moreover, both the lowest unoccupied molecular orbital (LUMO) and HOMO energy levels of the polymers were calculated (based on one repeat unit), which decreased due to the introduction of different numbers of fluorine. The LUMO levels were calculated to be −2.5, −2.57 and −2.6 eV for BTzDTBT, BTzDTFBT and BTzDT2FBT, respectively, and the HOMO levels were calculated to be −4.97, −5.06 and −5.09 eV for BTzDTBT, BTzDTFBT and BTzDT2FBT, respectively, showing a well matched trend with the measured data.

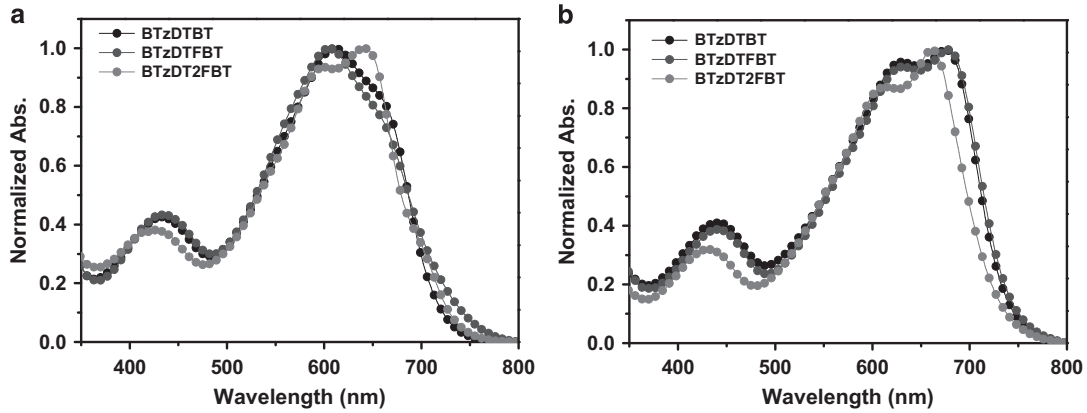

Figure 1 UV–vis absorption spectra of polymers in chloroform (**a**) and as a film (**b**). A full color version of this figure is available at *Polymer Journal* online.

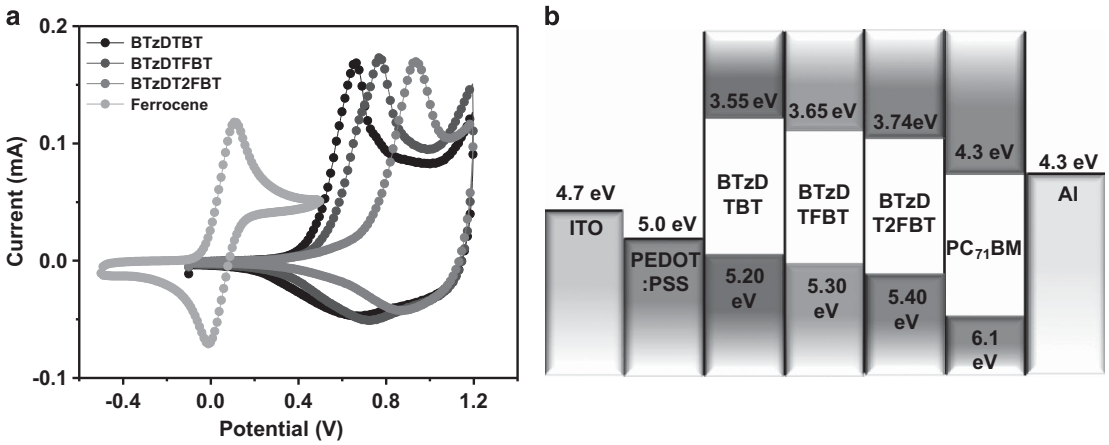

Figure 2 (**a**) Cyclic voltammograms of polymers and (**b**) energy band diagram. A full color version of this figure is available at *Polymer Journal* online.

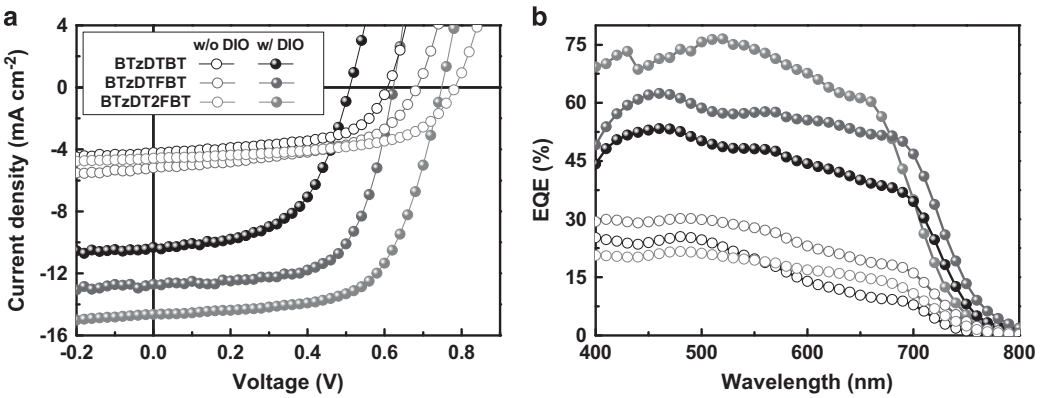

Figure 3 (**a**) *J–V* characteristics and (**b**) EQE spectra of polymer:$PC_{71}BM$ PSCs with and without DIO. A full color version of this figure is available at *Polymer Journal* online.

The three copolymers showed good solubility in common organic solvents, such as chloroform (CF) and chlorobenzene (CB). The number average molecular weights were determined to be 19 (PDI = 2.5), 23 (2.6) and 27 kDa (3.5) for BTzDTBT, BTzDTFBT, BTzDT2FBT, respectively (Table 1). The molecular weight and PDI were measured by gel permeation chromatography using *o*-dichlorobenzene as the eluent at 80 °C. The thermal properties of the polymers were analyzed by TGA and DSC measurements. BTzDTBT, BTzDTFBT and BTzDT2FBT showed similar decomposition temperatures (T_d) of 334, 335 and 338 °C, respectively, at 5% weight loss. No thermal transitions were observed for all polymers in the DSC measurements in the range of 30–320 °C. (Supplementary Figure 2; Table 1).

Optical and electrochemical properties

Figure 1 shows the normalized UV–vis absorption spectra of BTzDTBT, BTzDTFBT and BTzDT2FBT in chloroform and as a film, and the resulting optical properties are summarized in Table 1. The three polymers exhibit broad light absorption covering 350–750 nm, with distinct high and low energy bands attributed to localized π–π^*

and internal charge transfer transitions. The absorption maximum (λ_{abs}) was measured at 611, 605 and 641 nm in chloroform, respectively, and at 675, 677 and 661 nm for BTzDTBT, BTzDTFBT and BTzDT2FBT films, respectively. Interestingly, BTzDT2FBT showed a pronounced shoulder peak at 641 nm in chloroform, indicating strong interchain interaction (or aggregation) due to enhanced interchain attraction even in solution. In the film, the spectra were red shifted and the shoulder peak was substantially intensified, relative to those in solution. The differences in the UV–vis spectra in solution and in film emphasized the facile interchain organization in the solid state. The optical band gaps were determined to be 1.66 eV for BTzDT2FBT and 1.65 eV for BTzDTBT and BTzDTFBT.

The introduction of fluorine substituents on BT decreased the HOMO and LUMO energy levels significantly due to its strong electronegativity. The HOMO levels were determined to be −5.20, −5.30 and −5.40 eV for BTzDTBT, BTzDTFBT and BTzDT2FBT, respectively, by cyclic voltammetry (Figure 2a). The LUMO levels were estimated to be −3.55, −3.65 and −3.74 eV for BTzDTBT, BTzDTFBT and BTzDT2FBT, respectively, from the HOMO values and the corresponding optical band gaps of the films (Table 1). The deep HOMO levels with fluorine substituents may contribute to an improvement in oxidational stability and V_{OC} in the photovoltaic devices. The resulting energy band structures are also summarized in Figure 2b.

Photovoltaic characteristics

To investigate the photovoltaic characteristics of three A_1–D–A_2 polymers, we fabricated conventional-type devices with a device configuration of ITO/ PEDOT:PSS/polymer:$PC_{71}BM$/Al. First, to optimize the device fabrication condition, the polymer:$PC_{71}BM$ blend ratio was varied from 2:1 to 1:4 (by weight). For all polymers, the optimized polymer:$PC_{71}BM$ blend ratio was found to be 1:1 (w/w) (Supplementary Figure 3; Supplementary Table 1). Figure 3a and b exhibit the current density (*J*)–voltage (V) characteristics and EQE spectra of the optimized devices at 1:1 blend ratio. The detailed photovoltaic parameters are listed in Table 2. Without any processing additives and post treatments, poor photovoltaic PCE of 1.49–2.08% was obtained for all devices. To optimize the device properties, we also tried to use several processing additives, such as 1,8-octanedithiol, diphenylether and DIO, with varying concentrations. As a result, the PSC devices processed with DIO (3 vol%) showed a remarkable enhancement in device performance. Processing additives have been widely used to control the nanoscale morphology of polymer:fullerene

Table 2 Photovoltaic characteristics of polymer:$PC_{71}BM$ (1:1 w/w) PSCs

Polymer	*Additive (3% DIO)*	J_{SC} *(mA cm^{-2})*	V_{OC} *(V)*	*FF*	*PCE (%)*	*[Cal.]* J_{SC} *(mA cm^{-2})*
BTzDTBT	No	4.20	0.61	0.58	1.49	3.83
	Yes	10.31	0.51	0.56	2.92	10.10
BTzDTFBT	No	5.18	0.69	0.53	1.86	5.48
	Yes	12.70	0.62	0.65	5.14	12.50
BTzDT2FBT	No	4.57	0.78	0.58	2.08	3.94
	Yes	14.64	0.75	0.64	7.00	14.07

Abbreviations: BTzDTBT, poly[(2-tetradecyl-5,6-bis(tetradecyloxy)-2H-benzo[d][1,2,3]triazole)-alt-(4,7-di(thiophen-2-yl)benzo[c][1,2,5]thiadiazole)]; BTzDTFBT, poly[(2-tetradecyl-5,6-bis (tetradecyloxy)-2H-benzo[d][1,2,3]triazole)-alt-(5-fluoro-4,7-di(thiophen-2-yl)benzo[c][1,2,5]thiadiazole)]; BTzDT2FBT, poly[(2-tetradecyl-5,6-bis(tetradecyloxy)-2H-benzo[d][1,2,3]triazole)-alt-(5,6-difluoro-4,7-di(thiophen-2-yl)benzo[c][1,2,5]thiadiazole)]; DIO, 1,8-diiodooctane; FF, fill factor; J_{SC}, short circuit current density; PCE, power conversion efficiency.

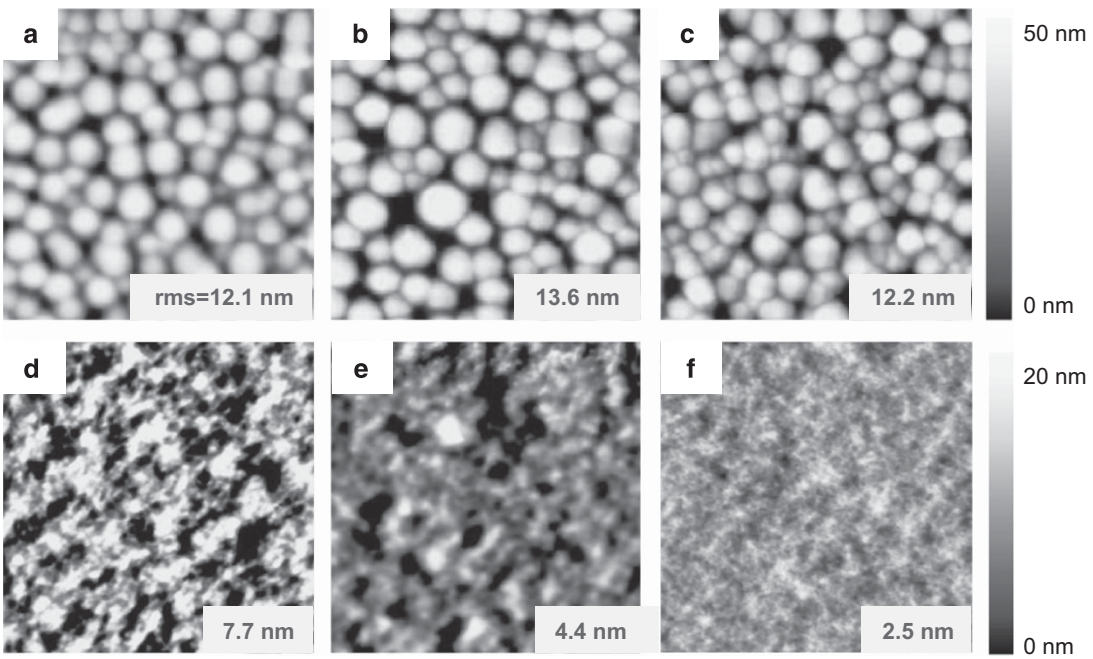

Figure 4 Atomic force microscopy topography images of blended films without (**a**–**c**) and with DIO (**d**–**f**) based on BTzDTBT (**a**, **d**), BTzDTFBT (**b**, **e**) and BTzDT2FBT (**c**, **f**). A full color version of this figure is available at *Polymer Journal* online.

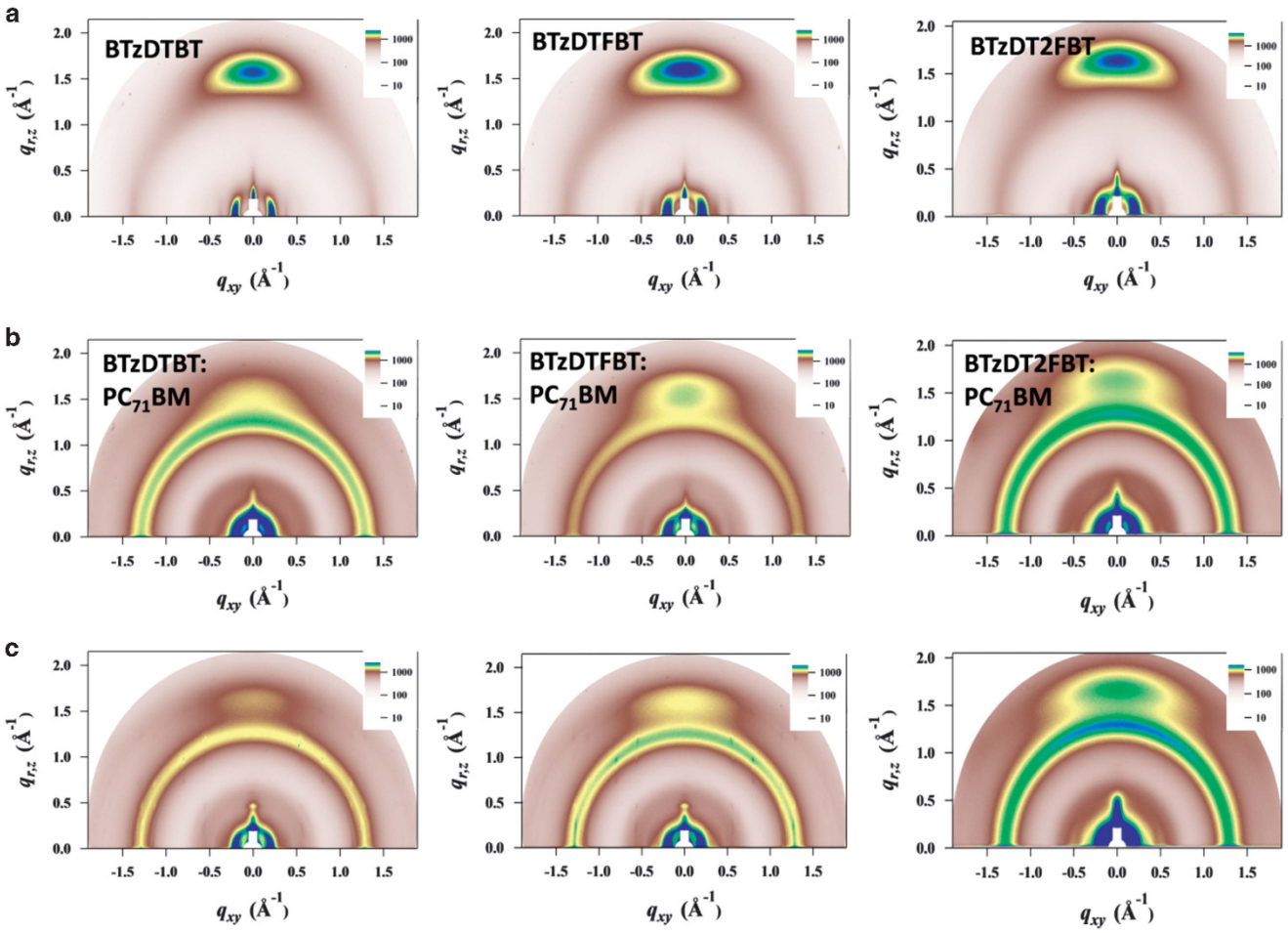

Figure 5 Two-dimensional GIWAXS images of (**a**) pristine polymers and polymer:$PC_{71}BM$ blend films (**b**) without and (**c**) with DIO. Left, middle and right panels show the images for BTzDTBT, BTzDTFBT and BTzDT2FBT, respectively.

BHJ blend films.[10] Considerable increases in J_{SC} were observed in all devices with DIO (BTzDTBT: 4.20 → 10.31 mA cm^{-2}, BTzDTFBT: 5.18 → 12.70 mA cm^{-2}, and BTzDT2FBT: 4.57 → 14.64 mA cm^{-2}). However, we observed that the introduction of DIO decreased V_{OC} for all devices. This may be attributed to a reduced effective band gap caused by improved crystallinity.[48,49] The V_{OC} gradually increased from 0.61 to 0.78 V with increasing number of fluorine atoms in the polymer backbone. The BTzDT2FBT:$PC_{71}BM$ device exhibited the highest PCE of 7% among the three copolymers with J_{SC} of 14.64 mA cm^{-2}, V_{OC} of 0.75 V and FF of 0.64. As shown in Figure 3b, the EQE values of the devices also increased by more than twofold with DIO, compared with those without DIO. The calculated J_{SC} values from the EQE curves matched well with the measured J_{SC} with an average error range of ~ 8%.

To investigate the remarkable improvements in device performance caused by the additive, we studied the morphology of polymer:$PC_{71}BM$ blend films by measuring the atomic force microscopy surface morphology. All blend films without DIO had high root-mean-square (r.m.s.) roughness of 12–14 nm and large phase segregation with a size of 100–300 nm in diameter (Figure 4). This morphology is expected to induce seriously geminate charge recombination, decline of exciton dissociation probability, and poor charge–carrier mobility by reducing the donor/acceptor interfacial area, thus leading to poor J_{SC} and FF.[50,51] In contrast, blend films with DIO had a more uniform surface. Among the blend films with 3% DIO, the blend film based on BTzDTBT still showed a very rough surface with r.m.s. roughness of 7.7 nm (Figure 4d). The most homogeneous and smooth surface morphology was observed in the BTzDT2FBT:$PC_{71}BM$ film (r.m.s. roughness = 2.5 nm). This supports the significant enhancement in the PCE of the device based on BTzDT2FBT with DIO.

Table 3 Hole and electron mobilities of BHJ devices from SCLC measurements

Active layer	μ_h ($cm^2 s^{-1} V^{-1}$)	μ_e ($cm^2 s^{-1} V^{-1}$)	μ_e/μ_h
BTzDTBT:$PC_{71}BM$	1.45×10^{-4}	1.31×10^{-4}	0.90
BTzDTFBT:$PC_{71}BM$	3.98×10^{-5}	3.02×10^{-5}	0.76
BTzDT2FBT:$PC_{71}BM$	7.29×10^{-5}	8.31×10^{-5}	1.14

Abbreviations: BTzDTBT, poly[(2-tetradecyl-5,6-bis(tetradecyloxy)-2H-benzo[d][1,2,3]triazole)-alt-(4,7-di(thiophen-2-yl)benzo[c][1,2,5]thiadiazole)]; BTzDTFBT, poly[(2-tetradecyl-5,6-bis (tetradecyloxy)-2H-benzo[d][1,2,3]triazole)-alt-(5-fluoro-4,7-di(thiophen-2-yl)benzo[c][1,2,5] thiadiazole)]; BTzDT2FBT, poly[(2-tetradecyl-5,6-bis(tetradecyloxy)-2H-benzo[d][1,2,3]triazole)-alt-(5,6-difluoro-4,7-di(thiophen-2-yl)benzo[c][1,2,5]thiadiazole)]; $PC_{71}BM$, phenyl-C71-butyric acid methyl ester.

We also investigated the correlation between intermolecular packing, molecular orientation and device performance by conducting GIWAXS. Figure 5 exhibits the two-dimensional GIWAXS images for pristine polymer and polymer:$PC_{71}BM$ blend films without and with DIO. In-plane and out-of-plane line-cuts and the detailed packing parameters extracted from GIWAXS profiles are also shown in

Supplementary Figure 4 and Supplementary Table 2. All of the pristine films showed a strong (100) laminar peak at $q_{xy} = 0.223–0.217$ Å^{-1} (d-spacing = 28.15–28.96 Å) in the in-plane direction and π–π stacking (010) peak at $q_z = 1.632–1.689$ Å^{-1} (d-spacing = 3.72–3.85 Å) in the out-of-plane direction, indicating a face-on orientation. Interestingly, increasing the number of fluorine substituents decreased the π–π stacking distance from 3.85 Å for BTzDTBT to 3.74 Å for BTzDTFBT and 3.72 Å for BTzDT2FBT. This implies stronger interchain packing between neighboring polymer chains via intermolecular S—F dipole–dipole interactions. After blending with $PC_{71}BM$, the π–π stacking (010) peak remains in the out-of-plane direction for all polymers, but the π–π stacking distance increased slightly for the BTzDTBT (3.87 Å) and BTzDTFBT (3.84 Å) blend films, in contrast to BTzDT2FBT (3.71 Å). This may be attributed to the partial disruption of interchain packing by mixing with $PC_{71}BM$.[52] Upon the addition of DIO, it can be noticed that all of the blend films showed reduced π-π stacking distances (BTzDTBT: 3.77 Å, BTzDTFBT: 3.80 Å, and BTzDT2FBT: 3.66 Å), implying a recovered strong interchain packing with DIO. Because the short π–π stacking distance and pronounced face-on orientation are beneficial to charge transport in the vertical direction in BHJ PSCs,[53] the GIWAXS results clearly support the remarkable J_{SC} enhancement by the introduction of DIO.

High charge–carrier mobility and balanced electron/hole carrier transport are considered important prerequisite conditions for high-performance photovoltaic devices. To quantify the charge–carrier mobilities, hole (μ_h) and electron (μ_e) mobilities of the BHJ PSCs with DIO were measured using the SCLC method (Supplementary Figure 5; Table 3). The average hole and electron mobilities were determined to be $\mu_h = 1.45 \times 10^{-4}$, 3.98×10^{-5} and 7.92×10^{-5} cm^2 V^{-1} s^{-1} and $\mu_e = 1.31 \times 10^{-4}$, 3.02×10^{-5} and 8.3×10^{-5} cm^2 V^{-1} s^{-1} for the BTzDTBT, BTzDTFBT and BTzDT2FBT BHJ devices, respectively. In the presence of DIO, all of the polymers showed well balanced ratios of electron/hole mobility in the range of 0.76–1.14, which can be beneficial for reducing charge recombination and enhancing J_{SC}.

CONCLUSION

In summary, three types of A_1–D–A_2 type π-conjugated copolymers were designed and synthesized based on the similarly structured BT and BTz as two electron-deficient moieties. The chemically versatile BTz unit was substituted with three tetradecyl or tetradecyloxy substituents, endowing solution processability without deteriorating the π-backbone planarity via intrachain S–O non-covalent coulombic interactions. Increasing the number of fluorine substituents on the BT unit decreased the frontier orbitals and enhanced the interchain packing between neighboring polymers via interchain S–F dipole–dipole interactions. BTzDT2FBT exhibited well intermixed semi-crystalline property with $PC_{71}BM$, smooth surface morphology, and face-on orientation of polymer backbones. As a result, the device based on BTzDT2FBT achieved the highest PCE of 7% among the three copolymers.

CONFLICT OF INTEREST

The authors declare no conflict of interest.

ACKNOWLEDGEMENTS

This work was supported by the National Research Foundation (NRF) of Korea (2015R1D1A1A09056905, 2015M1A2A2057506, 20100020209, 2015R1C1A1A02036599).

1 Chen, H.-Y., Hou, J., Zhang, S., Liang, Y., Yang, G., Yang, Y., Yu, L., Wu, Y. & Li, G. Polymer solar cells with enhanced open-circuit voltage and efficiency. *Nat. Photonics* **3**, 649–653 (2009).
2 Liu, Y., Zhao, J., Li, Z., Mu, C., Ma, W., Hu, H., Jiang, K., Lin, H., Ade, H. & Yan, H. Aggregation and morphology control enables multiple cases of high-efficiency polymer solar cells. *Nat. Commun.* **5**, 5293 (2014).
3 Zhao, J., Li, Y., Yang, G., Jiang, K., Lin, H., Ade, H., Ma, W. & Yan, H. Efficient organic solar cells processed from hydrocarbon solvents. *Nat. Energy* **1**, 15027 (2016).
4 Darling, S. B. & You, F. The case for organic photovoltaics. *RSC Adv* **3**, 17633–17648 (2013).
5 Sariciftci, N. S., Smilowitz, L., Heeger, A. J. & Wudl, F. Photoinduced electron transfer from a conducting polymer to Buckminsterfullerene. *Science* **258**, 1474–1476 (1992).
6 Xin, H., Subramaniyan, S., Kwon, T.-W., Shoaee, S., Durrant, J. R. & Jenekhe, S. A. Enhanced open circuit voltage and efficiency of donor–acceptor copolymer solar cells by using indene-C60 bisadduct. *Chem. Mater.* **24**, 1995–2001 (2012).
7 Krebs, F. C., Gevorgyan, S. A. & Alstrup, J. A roll-to-roll process to flexible polymer solar cells: model studies, manufacture and operational stability studies. *J. Mater. Chem.* **19**, 5442–5451 (2009).
8 Helgesen, M., Søndergaard, R. & Krebs, F. C. Advanced materials and processes for polymer solar cell devices. *J. Mater. Chem.* **20**, 36–60 (2010).
9 Park, J. K., Jo, J., Seo, J. H., Moon, J. S., Park, Y. D., Lee, K., Heeger, A. J. & Bazan, G. C. End-capping effect of a narrow band gap conjugated polymer on bulk heterojunction solar cells. *Adv. Mater.* **23**, 2430–2435 (2011).
10 Nguyen, T. L., Choi, H., Ko, S. J., Uddin, M. A., Walker, B., Yum, S., Jeong, J. E., Yun, M. H., Shin, T. J., Hwang, S., Kim, J. Y. & Woo, H. Y. Semi-crystalline photovoltaic polymers with efficiency exceeding 9% in a ~300 nm thick conventional single-cell device. *Energy Environ. Sci.* **7**, 3040–3051 (2014)
11 He, Z., Zhong, C., Su, S., Xu, M., Wu, H. & Cao, Y. Enhanced power-conversion efficiency in polymer solar cells using an inverted device structure. *Nat Photonics* **6**, 591–595 (2012).
12 Ye, L., Zhang, S., Zhao, W., Yao, H. & Hou, J. Highly efficient 2D-conjugated benzodithiophene-based photovoltaic polymer with linear alkylthio side chain. *Chem. Mater.* **26**, 3603–3605 (2014).
13 Huo, L., Liu, T., Sun, X., Cai, Y., Heeger, A. J. & Sun, Y. Single-junction organic solar cells based on a novel wide-bandgap polymer with efficiency of 9.7%. *Adv. Mater.* **27**, 2938–2944 (2015).
14 Choi, H., Ko, S. J., Kim, T., Morin, P. O., Walker, B., Lee, B. H., Leclerc, M., Kim, J. Y. & Heeger, A. J. Small-bandgap polymer solar cells with unprecedented short-circuit current density and high fill factor. *Adv. Mater.* **27**, 3318–3324 (2015).
15 Zhu, Z., Waller, D., Gaudiana, R., Morana, M., Mühlbacher, D., Scharber, M. & Brabec, C. Panchromatic conjugated polymers containing alternating donor/acceptor units for photovoltaic applications. *Macromolecules* **40**, 1981–1986 (2007).
16 Yuan, M.-C., Chiu, M.-Y., Chiang, C.-M. & Wei, K.-H. Synthesis and characterization of Pyrido[3,4-b]pyrazine-based low-bandgap copolymers for bulk heterojunction solar cells. *Macromolecules* **43**, 6270–6277 (2010).
17 Li, J., Ong, K. H., Sonar, P., Lim, S. L., Ng, G. M., Wong, H. K., Tan, H. S. & Chen, Z. K. Design and modification of three-component randomly incorporated copolymers for high performance organic photovoltaic applications. *Polym. Chem* **4**, 804–811 (2013).
18 Zhou, J., Xie, S., Amond, E. F. & Becker, M. L. Tuning energy levels of low bandgap semi-random two acceptor copolymers. *Macromolecules* **46**, 3391–3394 (2013).
19 Burkhart, B., Khlyabich, P. P. & Thompson, B. C. Semi-random two-acceptor polymers: elucidating electronic trends through multiple acceptor combinations. *Macromol. Chem. Phys.* **214**, 681–690 (2012).
20 Zhang, G., Fu, Y., Qiu, L. & Xie, Z. Synthesis and characterization of thieno[3,4-c] pyrrole-4,6-dione and pyrrolo[3,4-c]pyrrole-1,4-dione-based random polymers for photovoltaic applications. *Polymer* **53**, 4407–4412 (2012).
21 Jiang, J.-M., Chen, H.-C., Lin, H.-K., Lan, S.-C., Liu, C.-M., Yu, C.-M. & Wei, K.-H. Conjugated random copolymers of benzodithiophene–benzooxadiazole–diketopyrrolopyrrole with full visible light absorption for bulk heterojunction solar cells. *Polym. Chem.* **4**, 5321–5328 (2013).
22 Jung, J. W., Liu, F., Russell, T. P. & Jo, W. H. Semi-crystalline random conjugated copolymers with panchromatic absorption for highly efficient polymer solar cells. *Energy Environ. Sci.* **6**, 3301–3307 (2013)
23 Burkhart, B., Khlyabich, P. P. & Thompson, B. C. Influence of the acceptor composition on physical properties and solar cell performance in semi-random two-acceptor copolymers. *ACS Macro Lett.* **1**, 660–666 (2012).
24 Karakus, M., Apaydın, D. H., Yıldız, D. E., Toppare, L. & Cirpanet, A. Benzotriazole and benzothiadiazole containing conjugated copolymers for organic solar cell applications. *Polymer* **53**, 1198–1202 (2012).
25 Kotowski, D., Kotowski, D., Luzzati, S., Bianchi, G., Calabrese, A., Pellegrino, A., Po, R., Schimperna, G. & Tacca, A. Double acceptor D-A copolymers containing benzotriazole and benzothiadiazole units: chemical tailoring towards efficient photovoltaic properties. *J. Mater. Chem. A* **1**, 10736–10744 (2013).
26 Xiao, Z., Sun, K., Subbiah, J., Qin, T., Lu, S., Purushothaman, B., Jones, D. J., Holmes, A. B. & Wong, W. W. H. Effect of molecular weight on the properties and organic solar cell device performance of a donor– acceptor conjugated polymer. *Polym. Chem.* **6**, 2312–2318 (2015).
27 Wang, N., Chen, Z., Wei, W. & Jiang, Z. Fluorinated benzothiadiazole-based conjugated polymers for high-performance polymer solar cells without any processing additives or post-treatments. *J. Am. Chem. Soc.* **135**, 17060–17068 (2013).
28 Qin, T., Zajaczkowski, W., Pisula, W., Baumgarten, M., Chen, M., Gao, M., Wilson, G., Easton, C. D., Müllen, K. & Watkins, S. E. Tailored donor-acceptor polymers with an

A-D1-A-D2 structure: controlling intermolecular interactions to enable enhanced polymer photovoltaic devices. *J. Am. Chem. Soc.* **136**, 6049–6055 (2014).
29 Price, S. C., Stuart, A. C., Yang, L. Q., Zhou, H. X. & You, W. Fluorine substituted conjugated polymer of medium band gap yields 7% efficiency in polymer-fullerene solar cells. *J. Am. Chem. Soc.* **133**, 4625–4631 (2011).
30 Min, J., Zhang, Z. G., Zhang, S. Y. & Li, Y. F. Conjugated side-chain-isolated D-A copolymers based on Benzo[1,2-b:4,5-b′]dithiophene-alt-dithienylbenzotriazole: synthesis and photovoltaic properties. *Chem. Mater.* **24**, 3247–3254 (2012).
31 Min, J., Zhang, Z. G., Zhang, M. J. & Li, Y. F. Synthesis and photovoltaic properties of a D–A copolymer of dithienosilole and fluorinated-benzotriazole. *Polym. Chem.* **4**, 1467–1473 (2013).
32 Uy, R. L., Yan, L., Li, W. & You, W. Tuning fluorinated benzotriazole polymers through alkylthio substitution and selenophene incorporation for bulk heterojunction solar cells. *Macromolecules* **47**, 2289–2295 (2014)
33 Gao, L., Zhang, Z.-G., Xue, L., Min, J., Zhang, J., Wei, Z. & Li, Y. All-polymer solar cells based on absorption-complementary polymer donor and acceptor with high power conversion efficiency of 8.27%. *Adv. Mater.* **28**, 1884–1890 (2016).
34 Bin, H., Zhang, Z.-G., Gao, L., Chen, S., Zhong, L., Xue, L., Yang, C. & Li, Y. Non-fullerene polymer solar cells based on alkylthio and fluorine substituted 2D-conjugated polymers reach 9.5% efficiency. *J. Am. Chem. Soc.* **138**, 4657–4664 (2016).
35 Unay, H., Unlu, N. A., Hizalan, G., Hacioglu, S. O., Yildiz, D. E., Toppare, L. & Cirpan, A. Benzotriazole and benzodithiophene containing medium band gap polymer for bulk heterojunction polymer solar cell applications. *J. Polym. Sci. A Polym. Chem.* **53**, 528–535 (2015).
36 Yum, S., An, T. K., Wang, X., Lee, W., Uddin, M. A., Kim, Y. J., Nguyen, T. L., Xu, S., Hwang, S., Park, C. E. & Woo, H. Y. Benzotriazole-containing planar conjugated polymers with noncovalent conformational locks for thermally stable and efficient polymer field-effect transistors. *Chem. Mater.* **26**, 2147–2154 (2014).
37 Hou, J., Park, M.-H., Zhang, S., Yao, Y., Chen, L.-M., Li, J.-H. & Yang, Y. Bandgap and molecular energy level control of conjugated polymer photovoltaic materials based on Benzo[1,2-b:4,5-b′]dithiophene. *Macromolecules* **41**, 6012–6018 (2008).
38 Guo, X., Quinn, J., Chen, Z., Usta, H., Zheng, Y., Xia, Y., Hennek, J. W., Ortiz, R. P., Marks, T. J. & Facchetti, A. Dialkoxybithiazole: a new building block for head-to-head polymer semiconductors. *J. Am. Chem. Soc.* **136**, 1986–1996 (2013).
39 Guo, X., Kim, F. S., Jenekhe, S. A. & Watson, M. D. Phthalimide-based polymers for high performance organic thin-film transistors. *J. Am. Chem. Soc.* **131**, 7206–7207 (2009).
40 Schroeder, B. C., Huang, Z., Ashraf, R. S., Smith, J., D'Angelo, P., Watkins, S. E., Anthopoulos, T. D., Durrant, J. R. & McCulloch, I. Silaindacenodithiophene-based low band gap polymers-the effect of fluorine substitution on device performances and film morphologies. *Adv. Funct. Mater.* **22**, 1663–1670 (2012).
41 Zhang, Y., Chien, S.-C., Chen, K.-S., Yip, H.-L., Sun, Y., Davies, J. A., Chen, F.-C. & Jen, A. K.-Y. Increased open circuit voltage in fluorinated benzothiadiazole-based alternating conjugated polymers. *Chem. Commun.* **47**, 11026–11028 (2011).
42 Wang, Y., Parkin, S. R., Gierschner, J. & Watson, M. D. Highly fluorinated benzobisbenzothiophenes. *Org. Lett.* **10**, 3307–3310 (2008).
43 Babudri, F., Farinola, G. M., Naso, F. & Ragni, R. Fluorinated organic materials for electronic and optoelectronic applications: the role of the fluorine atom. *Chem. Commun.* **10**, 1003–1022 (2007).
44 Reichenbacher, K., Suss, H. I. & Hulliger, J. Fluorine in crystal engineering-"the little atom that could". *J. Chem. Soc. Rev.* **34**, 22–30 (2005).
45 Lee, W., Choi, H., Hwang, S., Kim, J. Y. & Woo, H. Y. Efficient conventional- and inverted-type photovoltaic cells using a planar alternating polythiophene copolymer. *Chemistry* **18**, 2551–2558 (2012)
46 Zhao, Y & Truhlar, D. G. The M06 suite of density functionals for main group thermochemistry, thermochemical kinetics, noncovalent interactions, excited states, and transition elements: two new functionals and systematic testing of four M06-class functionals and 12 other functionals. *Theor. Chem. Acc.* **120**, 215–241 (2008)
47 Zhao, Y. & Truhlar, D. G. Density functionals with broad applicability in chemistry. *Acc. Chem. Res.* **41**, 157–167 (2008)
48 Jo, J., Kim, S.-S., Na, S.-I., Yu, B.-K. & Kim, D.-Y. Time-dependent morphology evolution by annealing processes on polymer:fullerene blend solar cells. *Adv. Funct. Mater.* **19**, 866–874 (2009).
49 Vandewal, K., Gadisa, A., Oosterbaan, W. D., Bertho, S., Banishoeib, F., Severen, I. V., Lutsen, L., Cleij, T. J., Vanderzande, D. & Manca, J. V. The relation between open-circuit voltage and the onset of photocurrent generation by charge-transfer absorption in polymer: fullerene bulk heterojunction solar cells. *Adv. Funct. Mater.* **18**, 2064–2070 (2008).
50 Chen, H.-C., Chen, Y.-H., Liu, C.-C., Chien, Y.-C., Chou, S.-W. & Chou, P.-T. Prominent short-circuit currents of fluorinated quinoxaline-based copolymer solar cells with a power conversion efficiency of 8.0%. *Chem. Mater.* **24**, 4766–4772 (2012).
51 Liang, Y., Xu, Z., Xia, J., Tsai, S.-T., Wu, Y., Li, G., Ray, C. & Yu, L. For the bright future-bulk heterojunction polymer solar cells with power conversion efficiency of 7.4%. *Adv. Mater.* **22**, E135–E138 (2010).
52 Miller, N. C., Sweetnam, S., Hoke, E. T., Gysel, R., Miller, C. E., Bartelt, J. A., Xie, X., Toney, M. F. & McGehee, M. D. Molecular packing and solar cell performance in blends of polymers with a bisadduct fullerene. *Nano Lett.* **12**, 1566–1570 (2012).
53 Guo, X., Zhou, N., Lou, S. J., Smith, J., Tice, D. B., Hennek, J. W., Ortiz, R. P., Navarrete, J. T. L., Li, S., Strzalka, J., Chen, L. X., Chang, R. P. H., Facchetti, A. & Marks, T. J. Polymer solar cells with enhanced fill factors. *Nat. Photonics* **7**, 825–833 (2013)

Supplementary Information accompanies the paper on Polymer Journal website (http://www.nature.com/pj)